Proc. Natl. Acad. Sci. USA
Vol. 93, pp. 8208–8213, August 1996
Biochemistry

Location of a potential transport binding site in a sigma class glutathione transferase by x-ray crystallography

XINHUA JI*†, ERIC C. VON ROSENVINGE‡, WILLIAM W. JOHNSON‡, RICHARD N. ARMSTRONG‡§¶, AND GARY L. GILLILAND*¶

*Center for Advanced Research in Biotechnology, University of Maryland Biotechnology Institute, and National Institute of Standards and Technology, 9600 Gudelsky Drive, Rockville, MD 20850; ‡Department of Chemistry and Biochemistry, University of Maryland, College Park, MD 20742; and §Department of Biochemistry and Center in Molecular Toxicology, Vanderbilt University School of Medicine, Nashville, TN 37232

Communicated by David R. Davies, National Institute of Diabetes and Digestive and Kidney Diseases, Bethesda, MD, April 3, 1996 (received for review October 2, 1995)

ABSTRACT **The crystal structure of the sigma class glutathione transferase from squid digestive gland in complex with *S*-(3-iodobenzyl)glutathione reveals a third binding site for the glutathione conjugate besides the two in the active sites of the dimer. The additional binding site is near the crystallographic two-fold axis between the two α4-turn-α5 motifs. The principal binding interactions with the conjugate include specific electrostatic interactions between the peptide and the two subunits and a hydrophobic cavity found across the two-fold axis that accommodates the 3-iodobenzyl group. Thus, two identical, symmetry-related but mutually exclusive binding modes for the third conjugate are observed. The hydrophobic pocket is about 14 Å from the hydroxyl group of Tyr-7 in the active site. This site is a potential transport binding site for hydrophobic molecules or their glutathione conjugates.**

The glutathione transferases (EC 2.5.1.18) are a group of proteins involved in the biotransformation of endogenous and xenobiotic electrophilic compounds by catalyzing the addition of glutathione (GSH) to electrophilic functional groups. The enzymes are found in all eukaryotes and many bacteria. The soluble or cytosolic enzymes from vertebrates have been grouped into four distinct classes called alpha, mu, pi (1), and theta (2). Three-dimensional structures of isoenzymes of alpha (3), mu (4, 5), and pi (6–8) classes have been determined and support the unique classifications of the vertebrate proteins. The crystal structures of GSH transferases from other sources have been determined as well, including *Schistosoma japanicum* (9, 10), squid digestive gland (11), and the Australian blowfly (12). The latter enzyme is clearly related to the theta class enzymes that have representatives in vertebrates. The squid protein has been placed in a separate class, sigma, and does not appear to have a vertebrate analogue. Tainer and colleagues (10) have suggested that the *Schistosomal* enzyme belongs to a novel class of glutathione transferase with a distinct substrate repertoire. The genetic, structural, and mechanistic aspects of the glutathione transferases have been extensively reviewed (13–17).

Besides their catalytic role, several investigators have proposed that the proteins are also involved in the sequestration and intracellular transport of endogenous and xenobiotic molecules and perhaps their glutathione conjugates (18–20). These proposals have been based on the observation that many of the enzymes avidly bind hydrophobic molecules, as well as glutathione conjugates. Although the existence of specific binding sites for various ligands that are distinct from the active site has been proposed, little information about possible locations for these sites has been forthcoming. The one exception is the binding site for the antischistosomal drug praziquantel on the 26-kDa GSH transferase from *S. japanicum* that has been found by x-ray crystallography to be at the interface of the two subunits in the dimer (10). Glutathione conjugates (product analogues) have been found to bind exclusively at the active site of the enzymes, though the R-group appended to the sulfur may occupy different locations (14).

We report here the three-dimensional structure of the sigma class GSH transferase from squid digestive gland in complex with *S*-(3-iodobenzyl)glutathione (GSBzI) at 2.2-Å resolution. The heavy atom-bearing product analogue reveals the location of an additional glutathione conjugate binding site. Besides the two binding sites associated with the active sites in the dimer, a third binding site is found between the two subunits. This binding site is different in nature from the catalytic binding site because it has fewer specific hydrogen bonding interactions to the peptide and a unique hydrophobic cavity on the twofold axis of the dimer about 14 Å from the active site.

EXPERIMENTAL PROCEDURES

Crystallization of the Enzyme. The construction of the expression vector, the expression and purification of the recombinant enzyme, and the kinetic characterization of the enzyme were carried out as described (11). Cocrystallization experiments with GSBzI were initiated after discovering three heavy atom binding sites in the GSBzI derivative during the structure determination. The derivative was prepared by replacing the 1-(*S*-glutathionyl)-2,4-dinitrobenzene (GSDNB) with GsBzI in soaking experiments (11). Crystals, for the studies described here, were grown in sitting drops (15–30 μl) that initially consisted of between 6 and 8 mg of protein per ml in 25 mM Tris (pH 7.0) containing 1 mM EDTA, 2 mM GSBzI, and buffered (pH 7) ammonium sulfate at 40% saturation. The drops were equilibrated at 4°C against wells containing between 60% and 70% saturated ammonium sulfate (pH 7). Single crystals grew in 5–7 days.

X-Ray Data Collection and Data Processing. A crystal of the dimensions of 0.3 × 0.4 × 0.8 mm^3 was mounted in a thin-walled capillary tube with a diameter 0.7 mm. X-ray diffraction data were collected using a Siemens electronic area detector mounted on a 3-axis Supper oscillation camera controlled by a PCS microcomputer. The camera length was 119 mm. Each electronic frame was composed of counts summed over a 0.2° range in ω with exposure times of 120 s. The raw

The publication costs of this article were defrayed in part by page charge payment. This article must therefore be hereby marked "*advertisement*" in accordance with 18 U.S.C. §1734 solely to indicate this fact.

Abbreviations: GSH, glutathione; GSBzI, *S*-(3-iodobenzyl)glutathione; GSDNB; 1-(*S*-glutathionyl)-2,4-dinitrobenzene.

Data deposition: The atomic coordinates have been deposited in the Protein Data Bank, Chemistry Department, Brookhaven National Laboratory, Upton, NY 11973 (reference 2GSQ).

†Present address: Advanced BioScience Laboratories–Basic Research Program, National Cancer Institute–Frederick Cancer Research and Development Center, P.O. Box B, Frederick, MD 21702.

¶To whom reprint requests should be addressed.

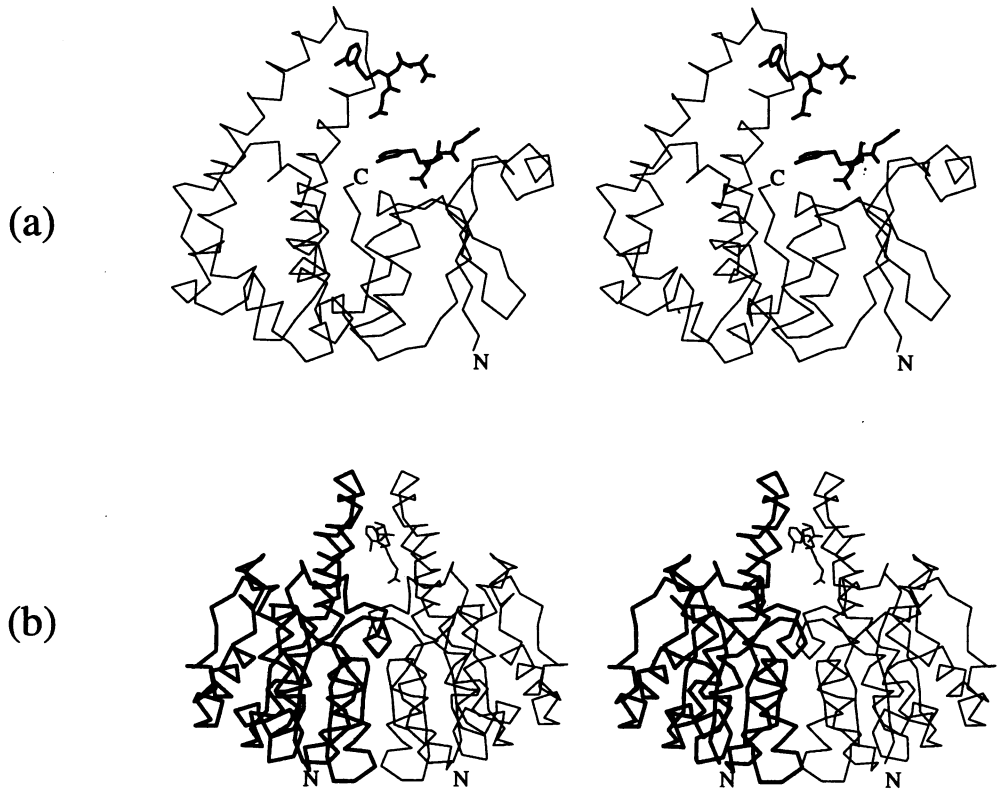

FIG. 1. (*a*) Stereoview of the C^{α} trace of one subunit of sigma class GSH transferase from squid digestive gland complexed with GSBzI. The GSBzI molecule in the lower position is in the catalytic binding site. The upper GSBzI molecule is at the dimer interface. (*b*) View of the primary GSBzI molecule at the subunit interface perpendicular to the two-fold axis of the dimer.

data frames were transferred from the PCS microcomputer to a Silicon Graphics (Mountain View, CA) Indigo2 computer for final processing. The data collection was carried out at controlled room temperature (19–20°C). The refinement of the unit cell parameters and the integration of reflection intensities were done with the XENGEN program system (21). Data were 99.7% complete up to 2.2 Å with a redundancy of 3.10. The average $I/\sigma(I)$ was 13.1 for all data and 1.9 for the shell between 2.34 and 2.20 Å.

Crystal Structure Determination. The starting model for the refinement was the polypeptide chain of the fully refined structure of the squid enzyme in complex with GSDNB (11) with the inhibitor and solvent molecules removed. After initial simulated annealing with X-PLOR (22), further refinement was carried out by using GPRLSA (23, 24) as previously described (11). The complete model of GSBzI in the active site was built into the $F_o - F_c$ map contoured at 3σ after one round of simulated annealing and model building followed by another round of least-squares refinement. Water molecules were found as $F_o - F_c$ peaks higher than 3σ and were added after six rounds of refinement and model adjustment. After the solvent structure was completed, the solvent molecules were checked against a series of omit maps with about 70 water molecules omitted each time. Another GSBzI molecule was then found between the two subunits on the crystallographic two-fold axis. A model built into the $F_o - F_c$ electron density map contoured at 1.5σ showed that the two-fold axis intersected the iodobenzyl group. Therefore, the two GSBzI molecules at the subunit interface were refined with atomic occupancy factors fixed at 0.5 to reflect the two mutually exclusive orientations. Model building, the examination of $2F_o - F_c$, $F_o - F_c$, and omit maps, the adjustment of the model and the incorporation of solvent molecules during refinement were done using the program O (25, 26).

RESULTS AND DISCUSSION

Overall Structure. The final coordinate set of the squid enzyme in complex with GSBzI consists of 202 amino acid residues, two GSBzI molecules (Fig. 1), one sulfate anion and 211 water molecules. The crystallographic R factor‖ for the model is 0.173 for 11,649 diffraction data between 6.0 and 2.2 Å with $I \geq 1\sigma(I)$. The root mean square deviation from ideal bond lengths and angle distances are 0.017 and 0.037 Å, respectively. The crystallographic coordinates for the structure have been deposited in the Brookhaven Protein Data Bank as entry 2GSQ.

The sigma class enzyme from squid is similar in overall structure to other soluble GSH transferases and consists of a smaller α/β domain (domain I) and a larger α domain (domain II) (Fig. 1*a*). Domain I, which constitutes roughly the first third of the protein, consists of a $\beta\alpha\beta\alpha\beta\beta\alpha$ structural motif that forms a mixed four-strand β-sheet in the order of 4312 with strand 3 antiparallel to the others. The domain is composed of three layers ($\alpha/\beta/\alpha$) with the central β-sheet sandwiched between α helices. The overall fold of domain I is classified as part of the thioredoxin superfamily fold which includes glutaredoxin, disulfide-bond formation facilitator, and glutathione peroxidase (27). Domain II of the protein is an all-α-helical domain composed of five α-helices (α4, α5, α6, α7, and α8) in a unique protein fold, the core of which consists of a bundle of four α-helices. Domain I is mainly responsible for glutathione binding while domain II constitutes part of the xenobiotic substrate binding site as has been discussed for other GSH transferases (4, 14, 16, 17).

Binding of GSBzI at the Active Site. The asymmetric unit consists of a single subunit with one GSBzI molecule bound in

‖Crystallographic $R = \Sigma_{hkl} \| |F_o| - |F_c| | / \Sigma_{hkl} |F_o|$ in which F_o and F_c are the observed and calculated structure factors, respectively.

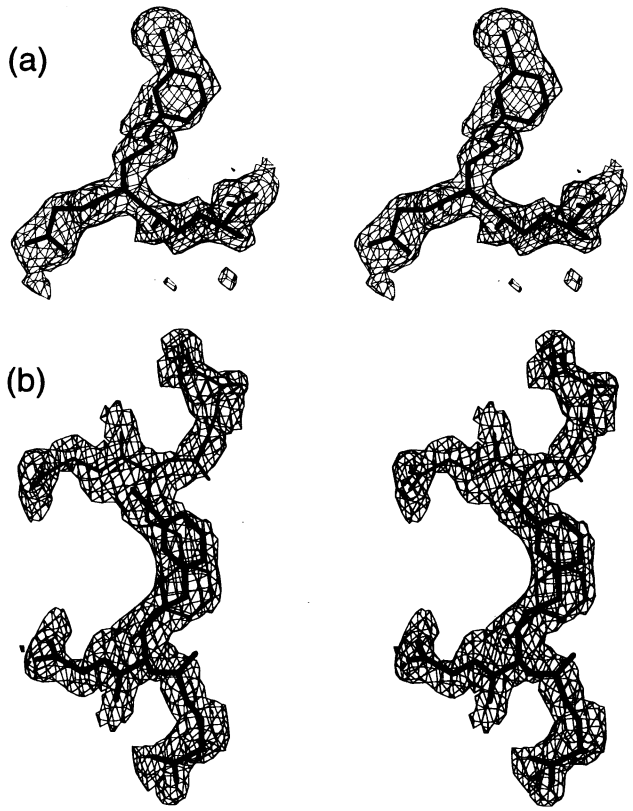

FIG. 2. (*a*) Stereoview of the $2F_o - F_c$ omit map of GSBzI molecule in the catalytic binding site of the squid glutathione *S*-transferase. The electron density map contoured at 1σ is illustrated in thin lines and the GSBzI molecule in thick lines. (*b*) Stereoview of the $2F_o - F_c$ omit map of the GSBzI molecule that is in the alternate binding site of the squid GSH transferase. The contour level of the electron density map is 0.5σ. The GSBzI molecule in thicker lines is the primary molecule, while the one in thinner lines is symmetry related to the primary molecule by the crystallographic two-fold axis.

the active site (Fig. 1*a*). A second GSBzI sits next to the α4-turn-α5 motif in domain II (Fig. 1*a*) on the crystallographic two-fold axis. The omit maps for the two GSBzI molecules in the asymmetric unit are shown in Fig. 2. The GSBzI molecule bound in the active site is anchored by specific hydrogen bonding interactions similar to those described for the enzyme in complex with GSDNB (11). The iodobenzyl moiety is tucked into a hydrophobic pocket defined by the side chains of F8, L10, R13, V102, and F106. The location of the iodobenzyl group is quite different from the location of the dinitrophenyl group in the complex with GSDNB, where the dinitrophenyl moiety points out of the hydrophobic pocket in a similar manner to the mu class M1–1 isoenzyme in complex with GSDNB. The "out" conformation is observed for those products that cannot adopt the "in" conformation because of steric clashes in the back of the xenobiotic binding pocket between its atoms and those of the protein (28). Thus, the binding of the R-groups of products can be classified into two general orientations, in and out as shown in Fig. 3. The only significant difference related to the two binding modes is the conformation of F106. The difference results from a 90° rotation about the CB—CG bond. Otherwise, the side-chain conformations of residues in the binding site are very well conserved.

Binding of GSBzI at the Dimer Interface. The biologically active dimer has three binding sites for GSBzI, one associated with each active site and a third at the subunit interface. The third GSBzI molecule is bound between and about 10 Å from the tips of the two α4-turn-α5 motifs at the dimer interface (Fig. 1*b*). Both the peptide and the iodobenzyl group lie across the crystallographic two-fold axis relating the two subunits in the dimer. That is, the ligand binds at two identical but mutually exclusive sites related by a two-fold axis. The iodobenzyl group is in a hydrophobic pocket formed by side chains from the α4-turn-α5 elements of both subunits while the glycyl end of the peptide points to the center of the dimer interface and the γ-glutamyl-end of the peptide protrudes on the other side of the two-fold toward the solvent. The hydrophobic interactions between the iodobenzyl group and the protein involve interactions with the subunit (subunit A) in the asymmetric unit and the crystallographically related subunit (subunit B). The hydrophobic pocket, shown in Fig. 4, is formed by the side chains of V115(A), V115(B), A107(A), A107(B), and the alkyl chain of K103(A). The peptidyl portion of GSBzI interacts through two hydrogen bonds with the protein. They include one between the main-chain carbonyl of A114(B) and the amino group of the γ-glutamyl residue and OD2 of N118(B) and the amide NH of the cysteinyl residue. The glycyl carboxylate, which points to the interior of the dimer, is hydrogen bonded to three water molecules (numbers 352, 376, and 391) and is surrounded by three positively charged groups within 4.6 Å, the ammonium groups of K103(A) and K103(B) and the guanidinium group of R13(A). This cationic cavity is important for the orientation of the glycyl-end of the peptide. The γ-glutamyl carboxylate has no direct interaction with the protein but is hydrogen bonded to waters 454 and 478.

The conformation of the GSBzI molecule bound between the two subunits is different from the one found in the active site as illustrated in Fig. 5. When the alignment is optimized by

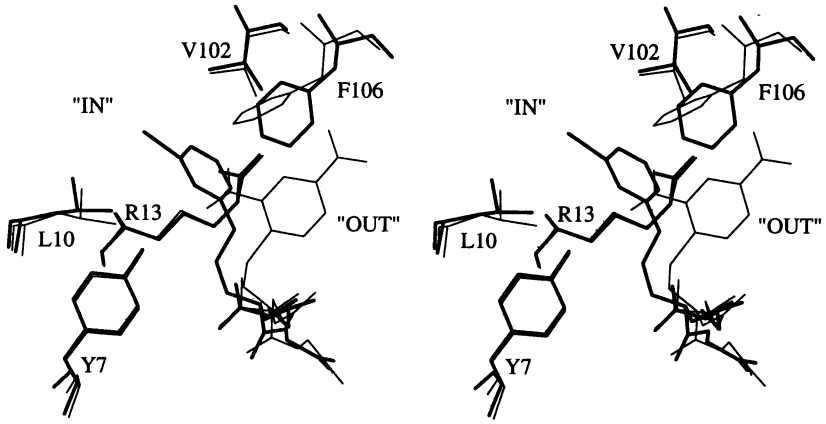

FIG. 3. Stereoview of a comparison of the xenobiotic binding site of sigma class GSH transferase with GSBzI (thick lines) and with GSDNB (thin lines) (11) bound. "IN" indicates inside the xenobiotic binding pocket, and "OUT" indicates the solvent channel inbetween the two subunits. Residue F8 is omitted for clarity.

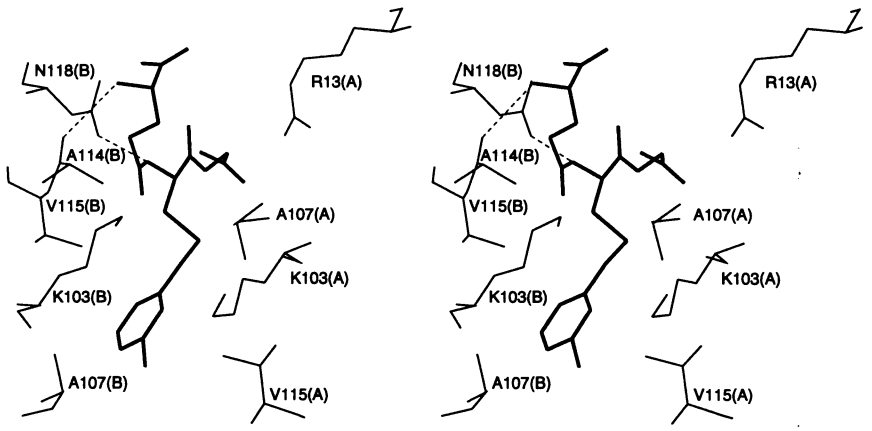

FIG. 4. Stereoview of the GSBzI molecule (thick lines) at the subunit interface of class sigma GSH transferase from squid. The ligand is about 10 Å from the tips of the two α4-turn-α5 motifs. The residues that interact with GSBzI are shown with thin lines and hydrogen bonds are shown with dashed lines. *A* and *B* indicate the dimer subunits A and B, respectively.

aligning the chiral centers of the cysteines, the conformational difference between the two molecules is quite apparent. Moreover, a significant distortion (≈37°) in the planarity of the γ-glutamyl peptide bond may be the result of steric interactions between peptide, the oxygen of A114 and the side chain of V115. Thus, the peptidyl portion of the third GSBzI molecule is not in a fully extended conformation as is the case when bound to the active site (Fig. 5).

The third binding site in the structure of the enzyme–GSDNB complex (1GSQ) (11) is not occupied with GSDNB. A structural comparison of the enzyme–GSDNB and the enzyme–GSBzI complexes offers an opportunity to determine whether the interfacial binding site exists because of, or is a result of, a conformational change in the protein. The root mean square deviation of C^{α} positions between the two structures 1GSQ and 2GSQ for all 202 target pairs is 0.35 Å, suggesting that there is no global change in the conformation of the protein upon binding GSBzI at the third binding site. However, the deviations in C^{α} positions for the ten residues (K105 to A114) that define the end of α4, the turn and the beginning of α5 are much higher. These residues move toward the crystallographic two-fold by an average of 1.1 Å. The largest differences in C^{α} positions are for A110 and A111 which move by 1.6 and 1.5 Å, respectively. The distance between the C^{α} of A110, which defines the tip of the α4-turn-α5 motif, and its symmetry related partner in the dimer decreases from 9.1 Å to 7.4 Å when the interfacial binding site is occupied as illustrated in Fig. 6. The net result is that the ends of the two helix-turn-helix elements in the dimer, like the prongs of a pair of tweezers, move toward one another by about 1.7 Å upon binding the third molecule of GSBzI. In addition, a total of three water molecules (406, 452, and 453 in 1GSQ) are displaced from the subunit interface (Fig. 6) and several changes in side-chain orientation occur upon binding the third molecule of GSBzI. Since the structure of the unliganded state of the enzyme has not been determined, it is not possible to tell if the differences in structure are due entirely to occupancy of the third binding site with GSBzI or if some are influenced by the type of ligand bound at the active site.

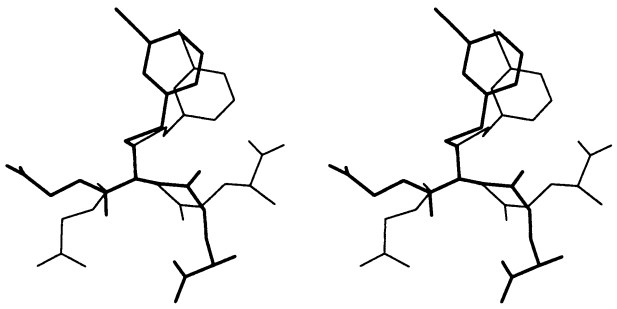

FIG. 5. Stereoview of the GSBzI molecule that is located between the two subunits of class sigma GSH transferase from squid (thick line) is compared with the GSBzI molecule bound in the active site (thin line). The alignment was optimized with respect to the chiral centers of the cysteine residues.

Dimerization and Ligand Binding Sites. The biologically active form of most known cytosolic GSH transferases is a dimer. The dimer interface is a potential site for the interaction of the protein with endogenous and xenobiotic ligands (18–20). This possibility was convincingly shown by the recent discovery that, at therapeutic concentrations, one molecule of the antischistosomal drug praziquantel binds at the inner part of the dimer interface in a groove adjoining the two catalytic sites of the 26-kDa *Schistosomal* GSH transferase. The dimer interfaces differ considerably among the various GSH transferase families, to the extent that heterodimers of subunits from different families are not observed (3, 11, 14). Each enzyme family represents a unique target for the binding of different ligands. This point is emphasized by the fact that the ligand and location of the interfacial binding site observed with the squid enzyme are quite different when compared with the enzyme–praziquantel complex.

Fig. 7 shows the structural alignment of the squid and *Schistosomal* GSH transferases in the subunit interface region. In the squid enzyme the third GSBzI molecule contacts the α4 helix (K103), the turn (F106 and A107) and the α5 helix (A114, V115, and N118). Whereas in the *Schistosomal* enzyme, the praziquantel molecule makes contacts with the α3 helix (Q67) and the α4 helix (G97, L100, D101, Y104, and R108). The only common position of contact is K103 in the squid enzyme that aligns with R108 of the *Schistosomal* protein (Fig. 7). The praziquantel molecule is lodged more deeply in the cavity between the subunits and is about 10 Å from the active site. The iodobenzyl group of GSBzI is about 14 Å from the active site. The two binding sites are clearly distinct in both their location and ligand binding properties.

Summary. The crevice formed by the association of GSH transferase subunits serves as a binding site for additional ligands including drugs (10) and glutathione conjugates. It will be of interest to see if the binding sites for many nonsubstrate ligands such as bilirubin, steroid hormones, and thyroid hormones (18–20, 31) involve the interfacial region between subunits. Finally, the existence of ligand binding sites at distinct locations in the dimer interfaces of different classes of GSH transferases suggests the possibility of developing unique

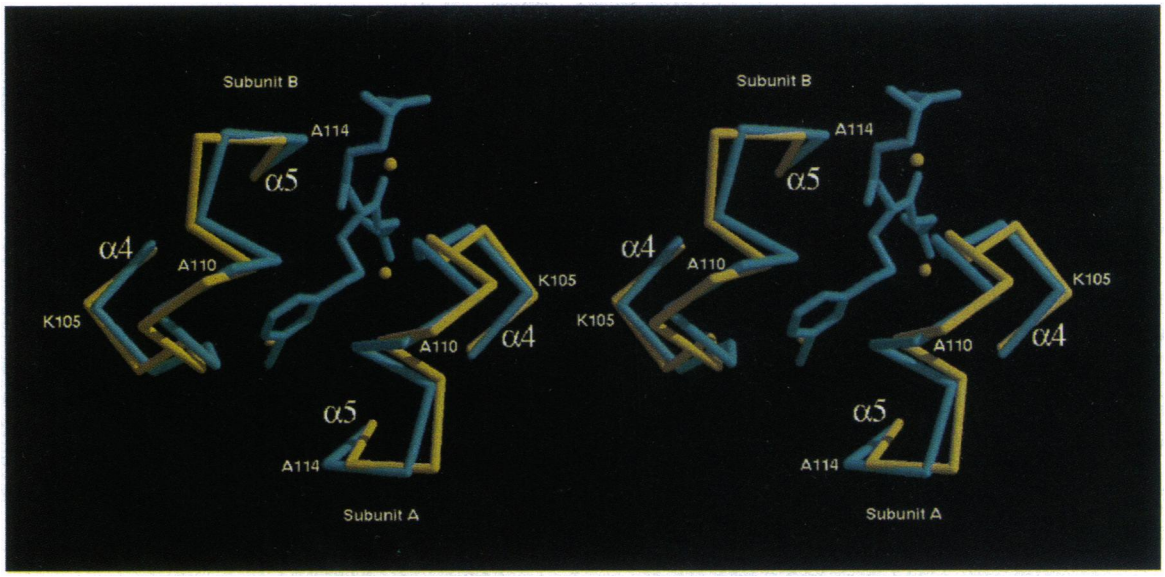

FIG. 6. RASTER3D (29) representation of the movement of the helix-turn-helix motif associated with occupancy of the interfacial binding site with GSBzI. The C^{α}-trace of the end (residues 105–114) of the helix-turn-helix motif for the enzyme in complex with GSDNB (1GSQ) in which the site is occupied by three water molecules is shown in yellow. The complex with GSBzI (2GSQ) is shown in blue.

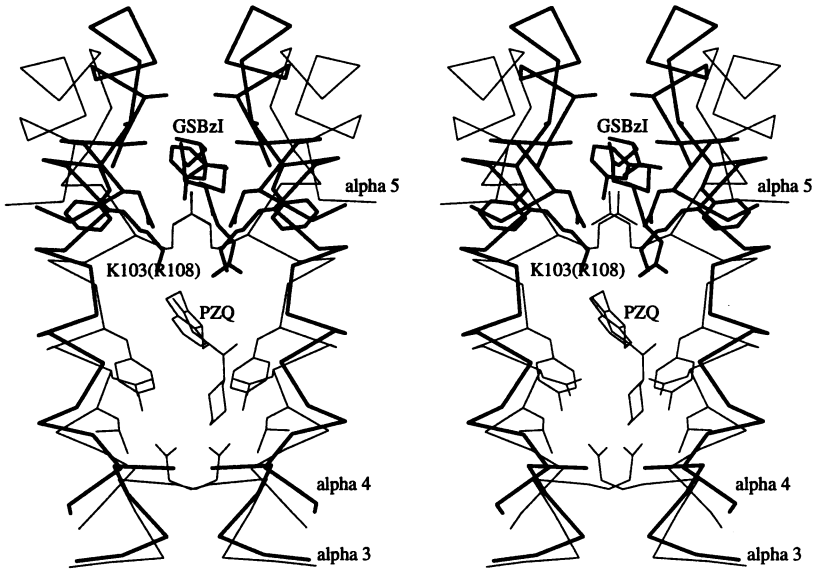

FIG. 7. Stereoview of the interface alignment of squid enzyme (2GSQ) (this work) and the *Schistosomal* enzyme (1GTB) (10) based on the alignment of all C^{α} positions of the proteins using the ALIGN program (30). Only the C^{α} trace of α3, α4 and α5, the six side chains for each protein that make contact with the non-substrate ligand praziquantel and the GSBzI molecule bound at the subunit interface are shown. The squid and *Schistosomal* enzymes are illustrated in the thick and thin lines, respectively.

isoenzyme-specific inhibitors for this group of enzymes targeted at the dimer interface.

We are grateful to Dr. S. Tomarev for providing the expression vector for the squid enzyme and to Dr. John Tainer for providing the coordinates of the GSH transferase–praziquantel structure before their release. This work was supported by a grant from the National Institutes of Health (GM30910).

1. Mannervik, B., Ålin, P., Guthenberg, C., Jensson, H., Tahir, M. K., Warholm, M. & Jornvall, H. (1985) *Proc. Natl. Acad. Sci. USA* **82,** 7202–7206.
2. Meyer, D. J., Coles, B., Pemble, S. E., Gilmore, K. S., Fraser, G. M. & Ketterer, B.(1991) *Biochem. J.* **274,** 409–414.
3. Sinning, I., Kleywegt, G. J., Cowan, S. W., Reinemer, P., Dirr, H. W., Huber, R., Gilliland, G. L., Armstrong, R. N., Ji, X., Board, P. G., Olin, B., Mannervik, B. & Jones, T. A. (1993) *J. Mol. Biol.* **232,** 192–212.
4. Ji, X., Zhang, P., Armstrong, R. N. & Gilliland, G. L. (1992) *Biochemistry* **31,** 10169–10184.
5. Raghunathan, S., Chandross, R. J., Kretsinger R. H., Allison, T. J., Penington C. J. & Rule, G. S. (1994) *J. Mol. Biol.* **238,** 815–832.
6. Reinemer, P., Dirr, H. W., Ladenstein, R., Schaffer, J., Gallay, O. & Huber, R. (1991) *EMBO J.* **10,** 1997–2005.
7. Reinemer, P., Dirr, H. W., Ladenstein, R., Huber, R., Lo Bello, M., Federici, G. & Parker, M. W. (1992) *J. Mol. Biol.* **227,** 214–226.
8. Garcia-Saez, I., Parraga, A., Phillips, M. F., Mantle, T. J. & Coll, M. (1994) *J. Mol. Biol.* **237,** 298–314.
9. Lim, K., Ho, J. X., Keeling, K., Gilliland, G. L., Ji, X., Rüker, F. & Carter, D. C. (1994) *Protein Sci.* **3,** 2233–2244.
10. McTigue, L. A., Williams, D. R. & Tainer, J. A. (1995) *J. Mol. Biol.* **246,** 21–27.
11. Ji, X., von Rosenvinge, E. C., Johnson, W. W., Tomarev, S. I., Piatigorsky, J., Armstrong, R. N. & Gilliland, G. L. (1995) *Biochemistry* **34,** 5317–5328.

12. Wilce, M. C. J., Board, P. G., Feil, S. C. & Parker, M. W. (1995) *EMBO J.* **14,** 2133–2143.
13. Armstrong, R. N. (1991) *Chem. Res. Toxicol.* **4,** 131–140.
14. Armstrong, R. N. (1994) *Adv. Enzymol. Related Areas Mol. Biol.* **69,** 1–44.
15. Rushmore, T. H. & Pickett, C. B. (1993) *J. Biol. Chem.* **268,** 11475–11478.
16. Dirr, H., Reinemer, P. & Huber, R. (1994) *Eur. J. Biochem.* **220,** 645–661.
17. Wilce, M. C. J. & Parker, M. W. (1994) *Biochim. Biophys. Acta* **1205,** 1–18.
18. Litwack, G., Ketterer, B. & Arias, I. M. (1971) *Nature (London)* **234,** 466–467.
19. Jakoby, W. B. & Habig, W. H. (1980) in *Enzymatic Basis of Detoxication*, ed. Jakoby, W. B. (Academic, New York), Vol. 2, pp. 63–94.
20. Listowsky, I., Abramovitz, M., Homma, H. & Niitsu, Y. (1988) *Drug Metab. Rev.* **19,** 305–318.
21. Howard, A. J., Gilliland, G. L., Finzel, B. C., Poulos, T. L., Ohlendorf, D. H. & Salemme, F. R. (1987) *J. Appl. Crystallogr.* **20,** 383–387.
22. Brünger, A. T. (1992) X-PLOR Manual (Yale Univ. Press, New Haven, CT), Version 3.1, 187–218.
23. Furey, W., Wang, B. C. & Sax, M. (1982) *J. Appl. Crystallogr.* **15,** 160–166.
24. Hendrickson, W. (1985) in *Crystallographic Computing*, eds. Sheldrick, G., Kruger, C. & Goddard, R. (Clarendon, Oxford), Vol 3, pp. 306–311.
25. Jones, T. A., Zou, J.-Y., Cowan, S. W. & Kjeldgaard, M. (1991) *Acta Crystallogr. A* **47,** 110–119.
26. Jones, T. A. & Kjeldgaard, M. (1993) O Manual (Uppsala Univ., Uppsala, Sweden/Aarhus Univ., Aarhus, Denmark), Version 5.9.1.
27. Murzin, A. G., Brenner, S. E., Hubbard, T. & Chothia, C. (1995) *J. Mol. Biol.* **247,** 536–540.
28. Ji, X., Armstrong, R. N. & Gilliland, G. L. (1993) *Biochemistry* **32,** 12949–12954.
29. Bacon, D. J. & Anderson, W. F. (1988) *J. Mol. Graphics* **6,** 219–220.
30. Satow, Y., Cohen, G. H., Padlan, E. A. & Davies, D. R. (1986) *J. Mol. Biol.* **190,** 593–604.
31. Ishigaki, S., Abramovitz, M. & Listowsky, I. (1989) *Arch. Biochem. Biophys.* **273,** 265–272.